

# Ambient and elevated temperature mechanical properties of hot-pressed fused silica matrix composite

D.C. Jia\*, Y. Zhou, T.C. Lei

*School of Materials Science and Engineering, Harbin Institute of Technology, Harbin 150001, PR China*

Received 15 January 2002; accepted 28 April 2002

## Abstract

The ambient and elevated temperature mechanical properties of two kinds of hot-pressed fused silica matrix composites, SiO<sub>2</sub> + 5 vol.% Si<sub>3</sub>N<sub>4</sub> and SiO<sub>2</sub> + 5 vol.% Si<sub>3</sub>N<sub>4</sub> + 10 vol.% C<sub>f</sub>, were investigated. Si<sub>3</sub>N<sub>4</sub> additions greatly enhanced the ambient strength and fracture toughness, while, further incorporation of chopped carbon fibers only but sharply increased the fracture toughness value from 1.22 to 2.4 MPa m<sup>1/2</sup>. The strength of the two composites synchronously exhibited anomalous gains at certain elevated temperature range especially from 1000 to 1200 °C, and reached their maximum values at 1000 °C, 168.9 and 130.6 MPa, which were 77.0 and 77.4% higher than their ambient strength, respectively. The two composites exhibited catastrophic fracture even at 1000 °C, but manifested prominent plastic deformation at 1200 °C and usually no fracture occurred during the strength test. Vickers' indentation crack propagation behavior, combined with fractographs studies, suggested that toughening from carbon fiber was attributed primarily to the fiber bridging, pull-out and crack deflection.

© 2002 Elsevier Science Ltd. All rights reserved.

*Keywords:* Composites; Mechanical properties; SiO<sub>2</sub>; Si<sub>3</sub>N<sub>4</sub>; Toughening

## 1. Introduction

Fused silica is an essential material for many engineering applications because of its prominent properties, such as, characteristically low thermal expansion coefficient, low thermal conductivity, high softening temperature, excellent chemical inertness, low dielectric dissipation fraction and high dielectric strength, etc. For aerospace applications, where reliability should be the first considered factor, monolithic fused silica is rarely used due to its intrinsic brittleness and very low fracture strain.<sup>1</sup> Thus, continuous fibers particularly carbon and silica fibers are generally used as the reinforcements.<sup>1–4</sup> The carbon or silica fibers are usually used in form of unidirectional state, two dimensional cloth and three or multi-directional woven truss, fracture strain and fracture work can be dramatically increased,<sup>4</sup> and thus catastrophic fracture are avoided. Yet, as a result, some shortages are generated, such as, relative low density, low bending strength, intrinsic property anisotropy,

poor processing reproducibility and very high final cost. These problems can be readily solved if short fibers, whiskers or particles rather than the continuous fibers are used as reinforcements since traditional Powder Metallurgical (PM) processing technique can be used. Some studies have been done on fused silica matrix composites reinforced by Si<sub>3</sub>N<sub>4</sub><sup>5,6</sup> and BN<sup>7</sup> particle, SiC and Si<sub>3</sub>N<sub>4</sub> whisker, short carbon fiber,<sup>8</sup> aluminoborosilicate fiber<sup>9</sup> or fused silica fiber<sup>10,11</sup> etc., and many exhilarating results have been achieved. So far, however, the elevated temperature mechanical properties are rarely reported, which are also very important for engineering applications. Thus, in this paper, the bending strength as well as the bending fracture behavior with increasing temperature of fused silica matrix composites incorporated Si<sub>3</sub>N<sub>4</sub> particles and with or without short carbon fiber are comparatively investigated.

## 2. Experimental procedure

Fused silica (SiO<sub>2</sub>) powder (99.9% in purity and ~7.5 μm in average diameter), α-silicon nitride (Si<sub>3</sub>N<sub>4</sub>) powder (99.5% in purity and ~0.5 μm in average diameter),

\* Corresponding author. Tel.: +86-451-6414291; fax: +86-451-6413922.

*E-mail address:* dcjia@mail.hrb.hl.cninfo.net (D.C. Jia).

chopped carbon fiber ( $C_f$ ) (which is less than 2 mm in length and 6–8  $\mu\text{m}$  in diameter) were used as the starting materials. They were blended to yield two compositions: (1)  $\text{SiO}_2 + 5 \text{ vol.}\% \text{ Si}_3\text{N}_4$ ; (2)  $\text{SiO}_2 + 5 \text{ vol.}\% \text{ Si}_3\text{N}_4 + 10 \text{ vol.}\% \text{ Cf}$ .  $\text{Si}_3\text{N}_4$  powder was incorporated into  $\text{SiO}_2$  matrix powder by conventional wet ball milling method. Chopped  $C_f$  was pre-deconglomerated by a supersonic vibrator in ethanol, and blended with the wet ball milled  $\text{SiO}_2 + \text{Si}_3\text{N}_4$  suspension, then directly dried using a boiler in air atmosphere. During the drying process, the slurry was stirred slowly but continually to avoid or mitigate powder sedimentation too quickly till the slurry lost its fluidity. Finally, the two kinds of dried composite powders were hot-pressed in a vacuum atmosphere better than  $10^3$  Torr to obtain highly densified composites.

Flexural strength were tested at room temperature, 800, 1000 and 1200  $^\circ\text{C}$  in air, using four-point loading with outer and inner spans of 40 and 20 mm, respectively, at a crosshead rate of 0.5 mm/min. The dimensions of the flexure specimens were 3 mm  $\times$  4 mm  $\times$  50 mm. Single-edge-notched-beam (SENB) samples were fabricated by notching the segments of tested flexure specimens with a 0.15 mm thick diamond wafering saw. The SENB samples with dimensions of 2 mm  $\times$  4 mm  $\times$  20 mm were tested in three-point loading with a 16 mm span at a cross-head speed of 0.05 mm/min.

Vickers indentation crack propagation path and fractographs of the composites were observed on a scanning electron microscope (SEM) to obtain information about composites fracture characteristics needed for analyzing the toughening mechanisms.

### 3. Results and discussion

#### 3.1. Ambient temperature mechanical property

Room temperature mechanical properties testing results of the two composites including bending strength, Young's modulus, fracture toughness and fracture strain are summarized in Table 1. The ambient temperature Young's modulus for  $\text{SiO}_2 + 5 \text{ vol.}\% \text{ Si}_3\text{N}_4$  kept basically at the same level with that of the fused silica in spite of the stiffness of  $\text{Si}_3\text{N}_4$  ( $> 220 \text{ GPa}$ ) is much higher than that of the fused silica matrix. This may be due to its low addition content as well as its detrimental effect on the densification of the composite. In contrast, the flexural strength, fracture toughness and

fracture strain were sharply improved. The good strengthening and toughening effect from the addition of  $\text{Si}_3\text{N}_4$  particles was attributed to the crack deflection and microcracking induced by the  $\text{Si}_3\text{N}_4$  particles.<sup>12,13</sup>

When chopped short carbon fiber was incorporated, room temperature flexural strength of 10 vol.%  $C_f/\text{SiO}_2 + 5 \text{ vol.}\% \text{ Si}_3\text{N}_4$  composite was about 77% of the value for  $\text{SiO}_2 + 5 \text{ vol.}\% \text{ Si}_3\text{N}_4$ , which was similar to the strength change when chopped and milled aluminoborosilicate fiber was incorporated into slip-cast fused-silica composites reported by Lyons et al.<sup>9</sup> This was mainly attributed to the presence of fiber aggregates in 10 vol.%  $C_f/\text{SiO}_2$  composite, and it in turn led to the early failure of the composite at relatively lower stress or lower strain level than it could be since the fiber aggregates resulted in strength-reducing flaws. The composite Young's modulus was 58 GPa, which was at the same level with its matrix. This suggested that elastic stiffness improvement from the high modulus carbon fibers was de-compensated by the decreased relatively density of the composite due to the presence of the pores resulted from the fiber aggregates.

In spite of the strength and elastic stiffness changes, the fracture toughness achieved a very high value, 2.40  $\text{MPa m}^{1/2}$ , which was nearly twice of the value of the monolithic  $\text{SiO}_2 + 5 \text{ vol.}\% \text{ Si}_3\text{N}_4$  composite without carbon fiber. This was attributable to the fiber pull-out, fiber bridging and crack deflection<sup>14–18</sup> due to the reasonable bonding strength between carbon fibers and the matrix. So, it can be concluded that short carbon fiber tends to play an important role of toughening rather than strengthening for this composite matrix.

#### 3.2. Elevated temperature mechanical property

The curves of the two composites flexural strength vs. the testing temperature are shown in Fig. 1, and the elevated temperature strength values and their increasing rate compared with their room temperature strength values are summarized in Table 2. The trends in the flexural strength with increasing testing temperature were clearly shown. At 800  $^\circ\text{C}$ , the flexural strength of the two composites only slightly increased. At 1000  $^\circ\text{C}$ , the bending strength of the two composites got anomalous gains and reach their maximum values, 168.9 and 130.6 MPa, which were 77.0 and 77.4% higher than their ambient temperature strength values, respectively. As temperature further increased, the bending strengths

Table 1  
Room temperature mechanical properties of the fused silica matrix composites

Materials	Bending strength, $\sigma_b/\text{MPa}$	Young's modulus, $E/\text{GPa}$	Fracture toughness, $K_{IC}/\text{MPa m}^{1/2}$	Fracture strain, $\epsilon_f/\%$
$\text{SiO}_2 + 5 \text{ vol.}\% \text{ Si}_3\text{N}_4$	95.4	57.0	1.22	0.17
10 vol.% $C_f/\text{SiO}_2 + 5 \text{ vol.}\% \text{ Si}_3\text{N}_4$	73.2	58.0	2.40	0.13

slightly decreased, but even at 1200 °C, they still could retain very high values, 145.9 and 119.7 MPa, which were still 53.0 and 63.5% higher than their respective room temperature strength. The anomalous strength gain behavior of the two hot-pressed fused silica matrix composites at certain elevated temperature range is also reported on monolithic slip-cast fused-silica and its corresponding composites reinforced by aluminoborosilicate fiber<sup>9</sup> For example, the strength of the monolithic slip-cast fused-silica increased from 49.8 MPa at ambient temperature to 76.9 MPa at 1000 °C, with an increasing rate of about 54.4%. This kind of strength gain behavior at high temperature was attributed to increased atom mobility, which led to a limited amount of crack-tip blunting<sup>19</sup> and/or to the compressive stress states in the surface layer<sup>20</sup> relevant discussion on this topic will be made in a later paper. From the strength increasing rate values listed in the Table 2, it can be indicated that the composite added short carbon fibers seemed to have better heat resistance than the other one. This might be due to the better thermal stability of C<sub>f</sub>/SiO<sub>2</sub> interface than that of Si<sub>3</sub>N<sub>4</sub>/SiO<sub>2</sub> interface at high temperature, which is more beneficial to retain the reinforcement effect to higher temperature.

Furthermore, load-deflection curves recorded during the four-point-bending-strength test of the two composites

are shown in Fig. 2. At 1000 °C, where the highest strength values were exhibited, little plastic deformation was observed and the typical brittle fracture was exhibited for the two composites. In contrast, prominent plastic deformation was exhibited at 1200 °C for both of them due to the viscous flow of the fused silica matrix, and no fracture usually occurred for the specimens during four-point bending strength test till their tensile surfaces touched the upper surface of the clamp apparatus, so the bent specimens are still in good condition, typical morphologies of the tested specimens are shown in Fig. 3.

According to the above, it can be inferred that the brittle to plastic transition temperature ( $T_{b-p}$ ) of the two kinds of fused silica matrix composites corresponded to a certain temperature around 1200 °C. At a temperature lower than  $T_{b-p}$ , the intrinsic crack propagation stress operates the fracture of the composites, while, at a temperature higher than  $T_{b-p}$ , the plastic deformation stress determines the failure of the composites. At a temperature higher than  $T_{b-p}$ , though the strength value of the composites begin to decrease due to the dislocations movement, the fine Si<sub>3</sub>N<sub>4</sub> particles still can serve as effective obstacles for dislocations movement. Therefore, the composites can retain relatively much higher strength values at temperature higher than  $T_{b-p}$ . This

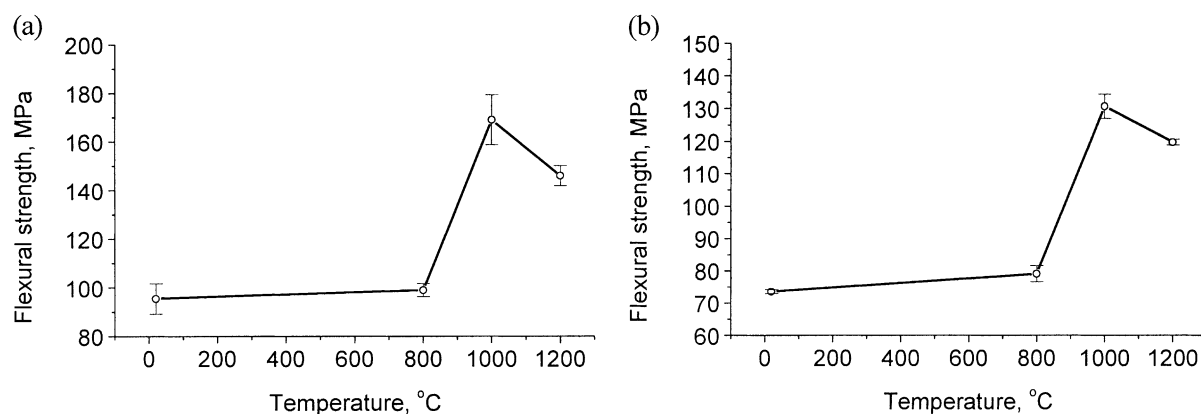


Fig. 1. Flexural strength vs. testing temperature of the two fused silica matrix composites: (a) SiO<sub>2</sub> + 5 vol.% Si<sub>3</sub>N<sub>4</sub>; (b) SiO<sub>2</sub> + 5 vol.% Si<sub>3</sub>N<sub>4</sub> + 10 vol.% C<sub>f</sub>.

Table 2

Elevated temperature flexural strength and increasing rate compared with their room temperature strength values of the fused silica matrix composites

Materials	Room temperature	800 °C	1000 °C	1200 °C
SiO <sub>2</sub> + 5 vol.% Si <sub>3</sub> N <sub>4</sub>	95.4	98.9 (3.6%) <sup>a</sup>	168.9 (77.0%)	145.9 (53.0%)
10 vol.% C <sub>f</sub> /SiO <sub>2</sub> + 5 vol.% Si <sub>3</sub> N <sub>4</sub>	73.6	79.1 (7.5%)	130.6 (77.4%)	119.7 (62.6%)

<sup>a</sup> Values in brackets are the increasing rates compared with their respective room temperature strength.

suggested that the strengthening effect from the  $\text{Si}_3\text{N}_4$  particles and carbon fiber didn't seem to be affected by the brittle to plastic transition of the fused silica matrix.

### 3.3. Indentation crack propagation path and fractograph observation

The Vickers' Indentation crack propagation path (shown in Fig. 4) and the room temperature fractographs (shown in Fig. 5) of the composites were characterized to explain the toughening mechanisms of carbon fibers at ambient temperature. As indicated, the crack propagation path was in a zigzagged shape (Fig. 4a and b) as a result of crack deflection from carbon fiber due to  $\text{C}_f/\text{SiO}_2$  interface debonding when carbon fibers were in relatively lower angles with the main crack plane, when the angle between a carbon fiber and the main crack plane is relatively higher, crack bridging (Fig. 4c) from the carbon fibers was usually observed.

Ambient fractograph observations of two composites showed that the fracture surfaces of  $\text{SiO}_2 + 5 \text{ vol.}\% \text{ Si}_3\text{N}_4$  composite were relatively flat and smooth (Fig. 5a), while, the composite containing carbon fibers exhibited much rougher fracture surface with many pulled-out carbon fibers, holes resulted from the pull-out carbon fibers as well as the grooves left by the debonded fibers (Fig. 5b). This was in good agreement with the observed results about the indentation crack propagation path, hence, it can be concluded that the fiber bridging, fiber pull-out as well as crack deflection induced by carbon fibers were the dominating toughening mechanisms of the composites at ambient temperature. It should also be noted that all the above were based on the 'weak' interface between the carbon fiber and the fused silica matrix, just as Evans<sup>21</sup> has pointed out that 'weak' interface is a prerequisite for attainment of fracture resistances that appreciably exceed those of the matrix.

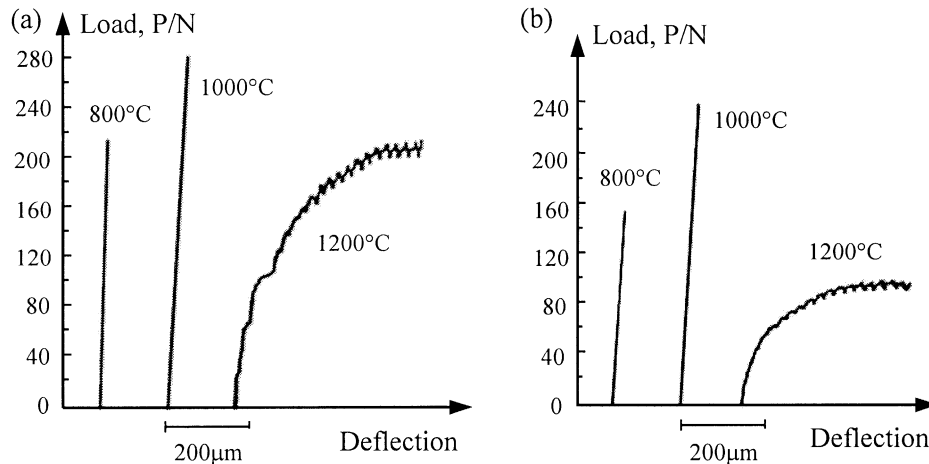


Fig. 2. Load-deflection curves of the fused silica composites corresponding to their flexural strength tests at different temperature: (a)  $\text{SiO}_2 + 5 \text{ vol.}\% \text{ Si}_3\text{N}_4$ ; (b)  $\text{SiO}_2 + 5 \text{ vol.}\% \text{ Si}_3\text{N}_4 + 10 \text{ vol.}\% \text{ C}_f$ .

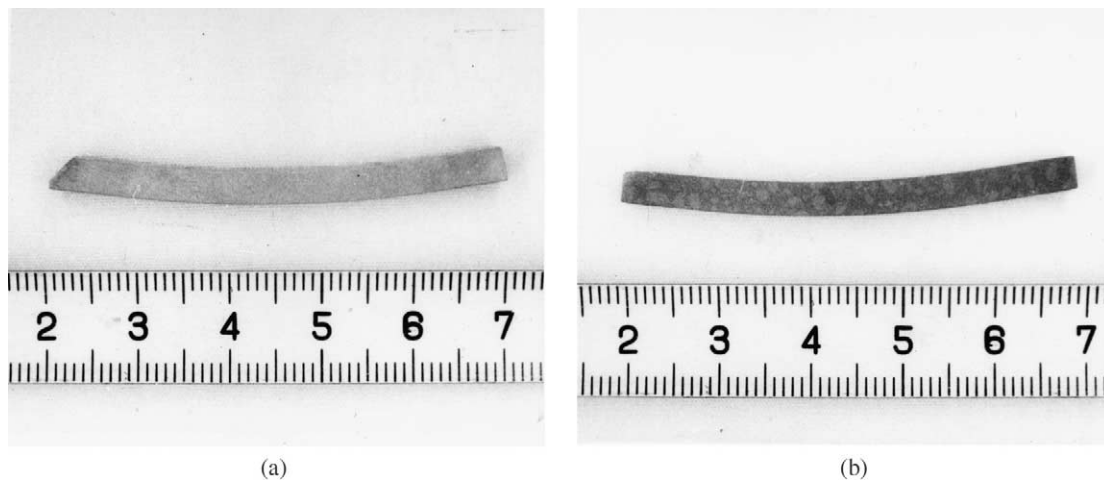


Fig. 3. Typical morphologies of the fused silica matrix composite samples after flexural strength test at 1200 °C: (a)  $\text{SiO}_2 + 5 \text{ vol.}\% \text{ Si}_3\text{N}_4$ ; (b)  $\text{SiO}_2 + 5 \text{ vol.}\% \text{ Si}_3\text{N}_4 + 10 \text{ vol.}\% \text{ C}_f$ .

Elevated temperature fractographs of the composites were observed. For  $\text{SiO}_2 + 5 \text{ vol.}\% \text{ Si}_3\text{N}_4$  composite fractured at  $1000^\circ\text{C}$ , the fractured surface (Fig. 6a) was only slightly rougher compared with the room temperature fractured surface (Fig. 5a), this was in consistent with their identical catastrophic failure manner. For the composites with carbon fibers addition, however, the fracture surface was scattered with many grooves and holes resulted from that the carbon fibers had been burned out during the sample stayed at the high testing temperature in air.

As aforementioned, the two composites samples exhibited apparent plastic deformation when they were tested at  $1200^\circ\text{C}$  and no fracture occurred. To know the oxidation degree of the carbon fibers at  $1200^\circ\text{C}$ , one

composite sample incorporated carbon fibers was arbitrarily selected and intentionally broken-off for SEM observation, typical fractographs are shown in Fig. 7. The oxidation of carbon fibers only took place in the surface layer of about  $150\text{--}180 \mu\text{m}$  in depth, and the fibers was completely burned out within the surface layer of  $100 \mu\text{m}$  in depth (Fig. 7a). Fig. 7b showed the morphology of the degraded carbon fibers partly oxidized and the increased interstice formed at the interface area between carbon fiber and the matrix. While, most carbon fibers in the composites still maintain their original state, and they were bonded very well with the matrix, Fig. 7c showed a typical morphology of the carbon fibers in good state. So, it can be suggested from the above that the reinforcement from carbon fibers

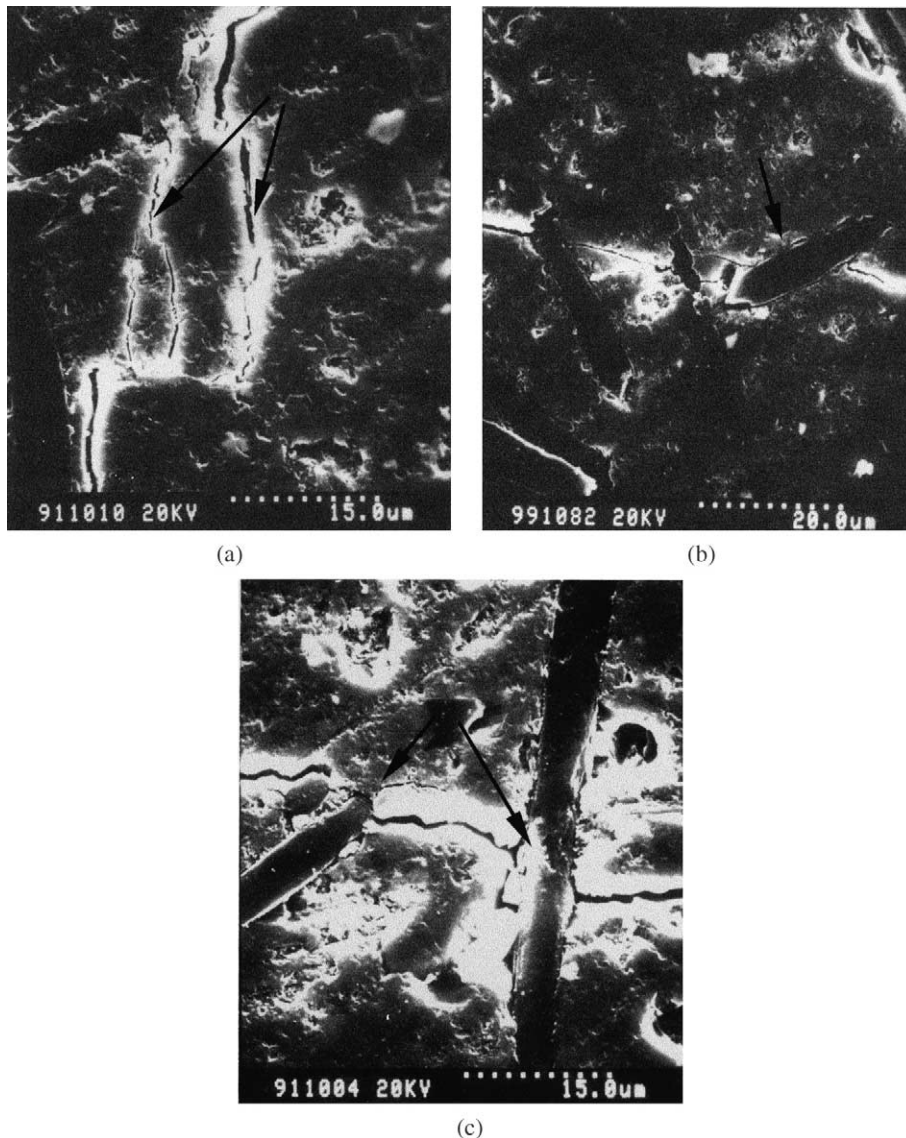


Fig. 4. SEM Vickers' indentation crack propagation path of 10 vol.%  $\text{C}_f/\text{SiO}_2 + 5 \text{ vol.}\% \text{ Si}_3\text{N}_4$  composite.

were affected slightly but not radically, and it was in good agreement with the elevated temperature strength testing results.

#### 4. Conclusions

1.  $\text{Si}_3\text{N}_4$  additions greatly enhanced the ambient temperature flexural strength and fracture toughness of the hot-pressed fused silica matrix composites, the additions of chopped short carbon fibers further increased the fracture toughness the values from 1.22 to 2.40  $\text{MPa m}^{1/2}$  due to the effective fiber bridging, pull-out and crack deflection toughening effects.
2. Both of the composites,  $\text{SiO}_2 + 5 \text{ vol.}\% \text{ Si}_3\text{N}_4$  and  $10 \text{ vol.}\% \text{ C}_f/\text{SiO}_2 + 5 \text{ vol.}\% \text{ Si}_3\text{N}_4$ , exhibited anomalous gains in strength at certain elevated temperature range especially at 1000–1200 °C. At 1000 °C, the flexural strength of the two composites reached their respective maximum values, 168.9 and 130.6 MPa, which were 77.0 and 77.4% higher than their respective ambient temperature strength.
3. At a temperature lower than or equal to 1000 °C, the two composites exhibited little plastic deformation and the failure belonged to a typical

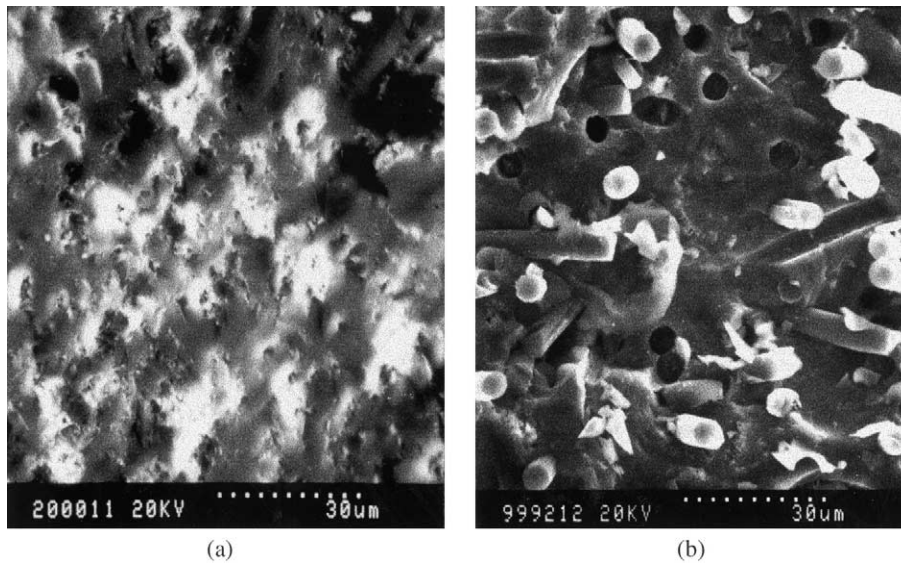


Fig. 5. Ambient SEM fractograph of  $\text{SiO}_2 + 5 \text{ vol.}\% \text{ Si}_3\text{N}_4$  (a) and  $10 \text{ vol.}\% \text{ C}_f/\text{SiO}_2 + 5 \text{ vol.}\% \text{ Si}_3\text{N}_4$  (b) composite.

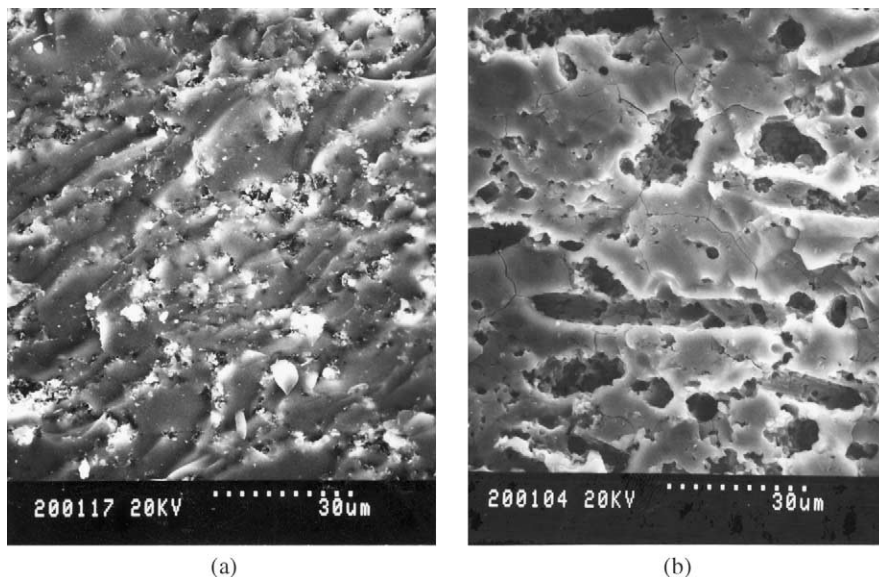


Fig. 6. Typical bending fractographs of  $\text{SiO}_2 + 5 \text{ vol.}\% \text{ Si}_3\text{N}_4$  (a) and  $10 \text{ vol.}\% \text{ C}_f/\text{SiO}_2 + 5 \text{ vol.}\% \text{ Si}_3\text{N}_4$  (b) composite tested at 1000 °C.

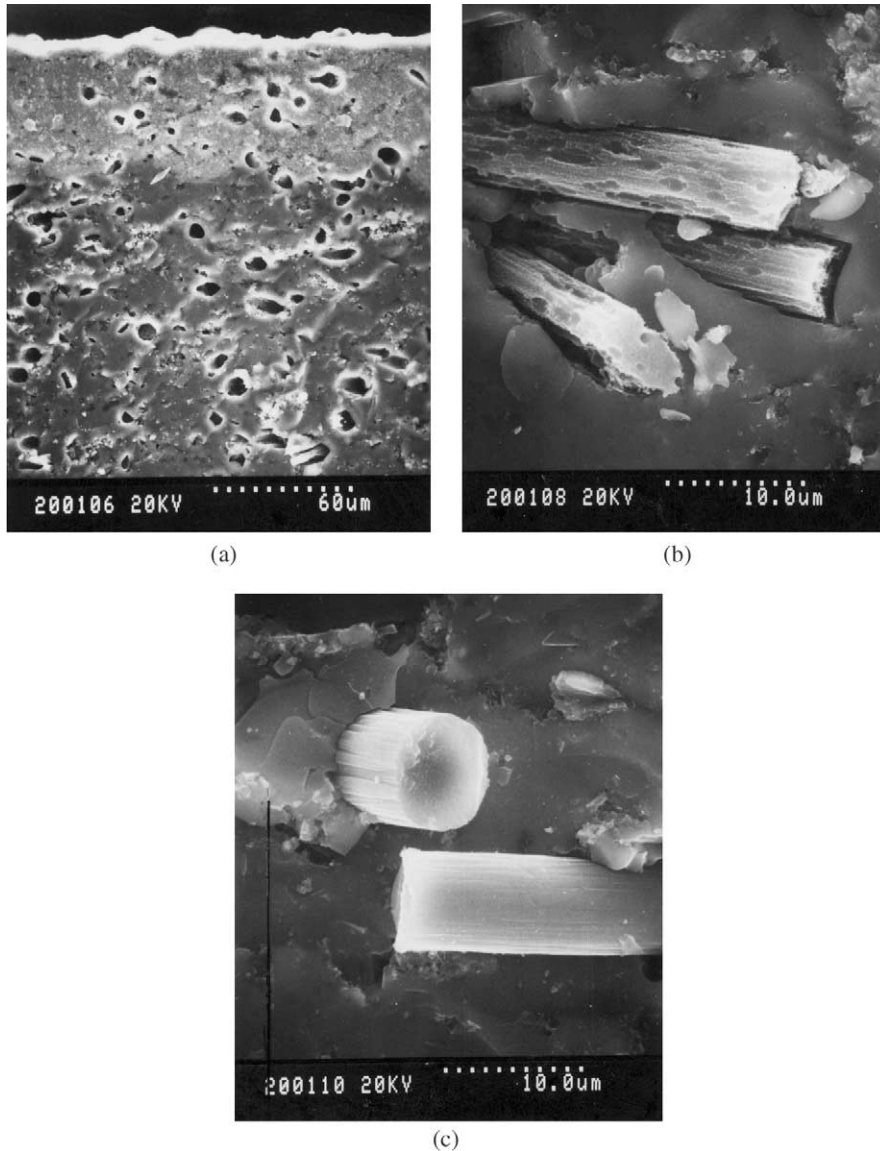


Fig. 7. SEM fractographs obtained at room temperature of 10 vol.%  $C_f/SiO_2 + 5$  vol.%  $Si_3N_4$  composite after flexural strength test at 1200 °C: (a) the carbon fibers in the shallow surface layer are completely burned out; (b) the partly oxidized carbon fiber situated near the surface layer; (c) the intact carbon fiber in the inner part of the samples.

brittle mode. In contrast, prominent plastic deformation was exhibited at 1200 °C for both of them and no fracture occurred for the specimens during four-point-bending strength test.

#### Acknowledgements

The authors wish to express their appreciation to Dr. S.H. Bai, at Northwestern Polytechnical University, for the elevated temperature mechanical property testing of the composites.

#### References

1. Yu, Q., *Materials Technology, Series of Missiles and Spaceflight—Materials and Technology (lower)*. Publishing House of Aerospace, Beijing, 1993 pp. 1–215.
2. Wu, G. T., Exploratory research on the applications of carbon fiber reinforced silica on the thermal-protective structure of satellite and aero-ship. *Aerospace Mater. Technol.*, 1991, **4**, 72–78.
3. Guo, J. K. and Huang, X. X., Dielectric ceramic composite. In *Second China–US Bilateral Seminar on Inorganic Materials Research Held in Gnithersberg, USA*, 1987, p. 110.
4. Guo, J. K. and Yan, T. S., *Microstructure and Properties of Ceramic Materials*. Beijing, Science Press, 1984 pp. 281–289.
5. Yao, J. J., Li, B. S., Huang, X. X. and Guo, J. K., Investigation on thermology properties and thermal shock resistance of  $SiO_2$ –

- Si<sub>3</sub>N<sub>4</sub> antenna window material. *J. Aeronautical Mater.*, 1996, **16**(3), 57–62.
6. Yao, J. J., Li, B. S., Huang, X. X. and Guo, J. K., Mechanical properties and its toughening mechanisms of SiO<sub>2</sub>–Si<sub>3</sub>N<sub>4</sub> composite. *J. Inorganic Mater.*, 1997, **12**(1), 47–53.
  7. Wen, G. W., Wu, G. L. and Lei, T. Q. *et al.*, Co-enhanced SiO<sub>2</sub>–BN ceramics for high-temperature dielectric applications. *J. Euro. Ceram. Soc.*, 2000, **20**, 1923–1928.
  8. Han, H. Q. *Microstructure and Properties of Several SiO<sub>2</sub> Matrix Composites*. Ms thesis, Harbin Institute of Technology, Harbin, 1995, pp. 47–50.
  9. Lyons, J. S. and Starr, T. L., Strength and toughness of slip-cast fused-silica composites. *J. Am. Ceram. Soc.*, 1994, **77**(6), 1673–1675.
  10. Meyer, F. P., Quinn, G. D. and Waick, J. C., Reinforcing fused silica with high-purity fibers. *Ceram. Eng. Sci. Proc.*, 1986, **6**(7), 646–656.
  11. Jia, D. C., Zhou, Y. and Lei, T. Q., Influences of hot-pressing process on the microstructure and mechanical properties of SiO<sub>2</sub>/SiO<sub>2</sub> composites. *Aerospace Mater. Technol.*, 2001, **31**(1), 29–31.
  12. Evans, A. G. and Faber, K. T., Toughening of ceramics by circumferential microcracking. *J. Am. Ceram. Soc.*, 1981, **64**, 394–398.
  13. Zhao, H. and Jin, Z. Z., The analysis of residual stress and toughening mechanisms of particulate reinforced dual-phase ceramics. *J. Chin. Ceram. Soc.*, 1996, **24**(10), 491–497.
  14. Faber, K. T. and Evans, A. G., Crack deflection process I: theory. *Acta Metall.*, 1983, **31**(4), 565–576.
  15. Becher, P. F. and Wei, G. C., Toughening behavior in SiC-whisker-reinforced alumina. *J. Am. Ceram. Soc.*, 1984, **67**(12), C267–C269.
  16. Becher, P. F., Hsueh, C. H. and Angelini, F. *et al.*, Toughening behavior in whisker-reinforced ceramic matrix composites. *J. Am. Ceram. Soc.*, 1988, **71**(6), 1050–1061.
  17. Becher, P. F., Microstructural design of toughened ceramics. *J. Am. Ceram. Soc.*, 1991, **74**(2), 255–269.
  18. Feng, Y., *Interface Structure of SiC Whisker Reinforced Oxide Based Ceramics and Its Effect on Mechanical Properties*. PhD thesis, Harbin Institute of Technology, Harbin, 1995, pp. 60–70.
  19. Brückner, R., Properties and structure of vitreous silica. *J. Non-Cryst. Solid*, 1970, **5**, 123–175.
  20. Rixecker, G., Wiedmann, I., Rosinus, A. and Aldinger, F., High-temperature effects in the fracture mechanical behavior of silicon carbide liquid-phase sintered with AlN–Y<sub>2</sub>O<sub>3</sub> additives. *J. Eur. Ceram. Soc.*, 2001, **21**, 1013–1019.
  21. Evans, A. G., Zok, F. W. and Davis, J., The role of interfaces in fiber-reinforced brittle matrix composites. *Comp. Sci. Technol.*, 1991, **42**, 3–24.